ISSN (Print) 1226-1750
ISSN (Online) 2233-6656
Journal of Magnetics 18(4), 460-465 (2013) http://dx.doi.org/10.4283/JMAG.2013.18.4.460

Permanent Magnet Motor Design for Turrets with Large Diameters

Ji-Young Lee[1]*, Dae-Suk Joo[1,2], Do-Kwan Hong[1], Shi-Uk Chung[1], Byung-Chul Woo[1], and Dae-Hyun Koo[1]

[1]*Korea Electrotechnology Research Institute, Changwon 642-120, Korea*
[2]*Pukyong National University, Busan 608-737, Korea*

(Received 2 September 2013, Received in final form 4 November 2013, Accepted 5 November 2013)

This paper deals with an approach for the initial design of a permanent magnet motor for turrets with large diameters. The proposed design techniques are introduced as three stages. The first is the selection of a pole-slot combination, the second is the selection of the rotor topology, and the last is choosing the outermost dimensions. In every stage, a useful technique is described with considerations for effective fabrication and motor performance, and magnetic field computation is performed using the finite element method.

Keywords : electric motor design, finite element methods, permanent magnet machines

1. Introduction

For electric motor designs, many researchers have introduced design examples using variable optimum algorithms [1-3]. However, an optimum design process using an optimum algorithm is usually used when there is already a prototype with performance almost satisfying the requirements. To improve the performance characteristics such as efficiency and torque ripple, optimum design processes are used, and the design variables are limited to detailed dimensions such as the magnet and tooth shapes. If optimum design processes are used in the initial design, in which parameters such as the inner and outer dimensions and the number of poles and slots are selected, there are too many design variables, and the process is time-consuming. To quickly define the initial dimensions of an objective motor prior to optimal design, proper assumptions and parametric designs considering the restrictions of fabrication and related systems are necessary [4, 5].

This paper presents a design approach for the initial design of a permanent magnet (PM) motor for turrets with large diameters, as a previous work of an optimum design introduced in [3]. The proposed design techniques are introduced as three stages. The first is the selection of the pole–slot combination, the second is the selection of the rotor topology, and the third is choosing the outermost dimensions. After introducing the specifications for the machine design, the three stages are explained in detail with some assumptions and restrictions considering fabrication. The design results are discussed with analysis and experimental results.

*Corresponding author: Tel: +82-55-280-1416
Fax: +82-55-280-1490, e-mail: jylee@keri.re.kr

2. Design Specifications

Table 1 shows the design specifications of a PM motor design for a turret application. The dimension constraints are only the maximum outer and minimum inner diameters. The required motor performance during a typical operating cycle is shown in Fig. 1. Even though the maximum torque in Fig. 1 is less than 5000 Nm, the required maximum torque for the design is 6000 Nm based on considerations for the starting torque, which must be greater than the running torque. In addition to these specifications, a motor that is as compact as possible is desired. Therefore, the system requirements must consider light weight, small

Table 1. Motor design specifications.

Quantity	Values and unit
Motor input voltage	388 Vrms/line
Max current	28.3Arms
Max output power	9 kW
Max torque	6000 Nm
Max speed	14.3 rpm
Torque ripple	Under 3%
Max outer diameter	2 m (including housing)
Minimum inner diameter	1.4 m (including housing)
Cooling	Natural cooling (enclosed condition)

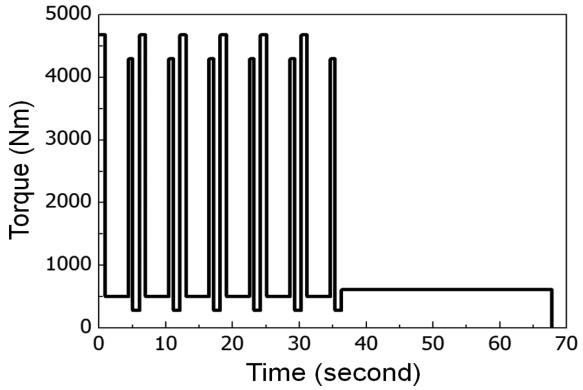

Fig. 1. Required motor performance during a typical operating cycle.

volume, and efficiency. Machine construction is chosen based upon the following considerations [6]:

1) External-rotor: Normally, with the same dimensions, external-rotor machines can provide higher torque density than internal-rotor machines, because the former can have a greater air-gap radius [7].

2) The shortest coils: Considering the limited machine volume, a double-layer concentrated winding is considered [8].

3. Selection of Pole-Slot Combinations

3.1. Pole-Slot Combinations Considered in Design

In the motor design process, it is very important to select the pole and slot number combinations that can achieve the highest machine performance [9]. In several literature surveys [8-12], the lowest common multiple (LCM), the winding factor, and an unbalanced magnetic pull (UMP) have been considered as the selection criteria. These factors were considered, and seven combinations were chosen with four ratios of pole and slot numbers (PSR), as listed in Table 2. The selection is made based on the following considerations:

1) Pole and slot numbers are varied from 120 to 240 and from 144 to 240, respectively. The interval of the pole number was 10.

2) The ratio of 360 and pole number, and the ratio of 360 and slot number are finite decimals for simple and clear blueprint work.

3) The greatest common divisor (GCD) of the pole and slot numbers is over 20 for the purpose of obtaining a relatively small analysis model to reduce the number of elements and the analysis time. The multi-symmetric model is ideally free from UMP.

4) The LCM between the number of poles and slots is over 400. The LCM order value increases the cogging torque frequency and reduces its magnitude [9].

Table 2. Poles-Slots Combinations considered in Design.

No. of pole \ PSR	2 : 3	4 : 3	5 : 6	8 : 9
240	-	180	-	-
200	-	150	240	225
150	225	-	180	-
120	-	-	144	-

3.2. Magnetic Field Analysis and Parameter Computations

To choose one combination, a surface-mounted PM (SPM) rotor is used as the basic rotor topology. In order to fairly compare between the models, some constraints have to be given:

1) The inner and outer diameters and axial length are fixed.

2) The slot open width is fixed to compare torque ripples.

3) The pole embraces are kept equal.

4) The maximum flux density in the middle of yoke and teeth in radial direction is kept below 1.8 T. The yokes and teeth dimensions are changed to obtain similar flux densities.

5) The slot fill factor is kept at about 50%.

To choose the coil specifications and core dimensions, classical analytical motor theory and equivalent magnetic circuit method are used. The tooth width, wire diameter, and number of conductors are decided for each model to obtain the highest efficiency under the maximum speed, as listed in Table 3.

The fundamental winding factor, k_w, for each model is taken from a previous study [12], because combinations with the same value of q, the number of slots per pole per phase, have the same winding factor [12].

For comparison, the electro-magnetic field computation of each model is performed by 2-dimensional finite element method (2-D FEM) using a commercial program, Maxwell. The motor performance regarding torque, core and copper losses, and efficiency are calculated with the electro-magnetic field analysis results. The related equations presented by Lee *et al.* are used [6], and the calculated results are also listed in Table 3.

The abbreviation Toq_cont is used to represent the torque constant defined as the ratio of the torque and the current. Curr_d is the current density defined as the ratio of the current and the area of wire.

3.3. Selection Method: Marking Score Technique

To select one combination through comparison analysis,

Table 3. The design results for pole-slot combinations.

PSR	2:3	4:3			**5:6**		8:9
Model name	150P 225S	200P 150S	240P 180S	120P 144S	**150P 180S**	200P 240S	200P 225S
No. of pole (NoP)	150	200	240	120	**150**	200	200
No. of slot (NoS)	225	150	180	144	**180**	240	225
NoP + NoS	375	350	420	264	**330**	440	425
LCM	450	600	720	720	**900**	1200	1800
Tooth width (mm)	14.0	11.0	9.0	21.0	**16.0**	11.8	12.5
Wire dia. (mm)	1.5	2.1	1.9	1.5	**1.6**	1.7	1.6
No. of Conductor	52	80	68	74	**64**	48	50
Fill factor (%)	50.7	51.7	48.1	49.8	**50.6**	50.5	48.0
Winding factor, k_w		0.866			**0.933**		0.945
Current (A)	22.4	35.7	34.4	24.7	**21.4**	24.9	24.7
Copper loss (kW)	5.0	6.7	6.8	6.7	**4.4**	4.6	4.5
Core loss (kW)	0.08	0.13	0.12	0.05	**0.07**	0.12	0.11
Torque (kNm)	5.7	6.2	5.9	6.1	**5.7**	5.9	5.8
Torque ripple (%)	7.7	7.1	7.9	1.8	**0.9**	0.6	1.4
Toq_cont (Nm/A)	254	173	171	247	**266**	237	235
Efficiency (%)	62.6	57.6	56.1	57.5	**65.4**	65.0	65.3
Curr_d (A/mm^2)	12.7	10.3	12.1	14.0	**10.6**	11.0	12.3

marking score techniques are used. The values of important parameters which influence the motor performance or fabrication are converted to the relative scores out of ten points, as shown in Table 4. Then, the model obtaining the highest total score is chosen. A weighting factor is considered according to the importance as presented by Lee *et al.* [5].

In Table 4, the scoring is classified into two sections. One is related to fabrication, and the other is for motor performance. The number of poles and slots is related to the cost and effort of fabrication. Since the split-core is essential for both the stator and rotor due to the large diameter, an increase of the number of poles and slots means an increase in the number of parts of the machine. Furthermore, the probability of winding error increases for a high number of slots. Therefore, in the fabrication, the score is higher if the model has fewer numbers of poles and slots, and a simpler winding pattern. The model 120P144S has the highest score and rank in the fabrication section, Rank-1.

For the motor performance, six parameters are considered. When the values of current, torque ripple, and current

Table 4. The scores of each parameter for pole-slot combinations.

PSR	2:3	4:3			**5:6**		8:9
Model name	150P 225S	200P 150S	240P 180S	120P 144S	**150P 180S**	200P 240S	200P 225S
NoP + NoS	7.0	7.5	6.3	10	**8.0**	6.0	6.2
Rank-1	**4**	**3**	**5**	**1**	**2**	**7**	**6**
Current	9.6	6.0	6.2	8.7	**10**	8.6	8.7
Torque	9.2	10	9.5	9.8	**9.2**	9.5	9.4
Torque ripple	0.8	0.8	0.8	3.3	**6.7**	10	4.3
Toq_cnst	9.6	6.5	6.4	9.3	**10**	8.9	8.8
Efficiency	9.6	8.8	8.6	8.8	**10**	9.9	10
Curr_d	8.1	10	8.5	7.4	**9.7**	9.4	8.4
Score_sum	46.9	42.1	40.0	47.3	**55.6**	56.3	49.6
Rank-2	**5**	**6**	**7**	**4**	**2**	**1**	**3**
Overall -Rank	**4**	**4**	**5**	**2**	**1**	**3**	**4**

density are converted, the reciprocal numbers of the values are considered. So, these values have high scores when their values are low. In contrast, the torque, torque constant, and efficiency have high scores when their values are high

Score_sum is the sum of the scores of the six parameters. Rank-2 is arranged in the order of higher Score_sum. In the motor performance section, Rank-2, the model 200P240S holds the first rank. Notably, the scores are high when models have high values of LCM and fundamental winding factor. However, this is just a tendency and not absolute, because of the non-linearity of magnetic material and the leakage flux paths of a magnetic circuit.

The Overall-Rank is the average of Rank-1 and Rank-2. Thus, the model 150P180S holds the first rank in the total models.

4. Selection of Rotor Topology

When the field-weakening performance is not considered, an SPM rotor has higher torque than any kind of interior PM (IPM) rotor [13]. If only considering the torque density, an SPM rotor is appropriate for turret applications. However, considering the possible external impact of the motor system, a protecting PM is required. As shown in Fig. 2, both the conventional and spoke-type IPM rotors are investigated. The spoke-type IPM rotor is selected since a large reluctance torque can compensate for the reduced PM torque, and it is more effective for manufacturing.

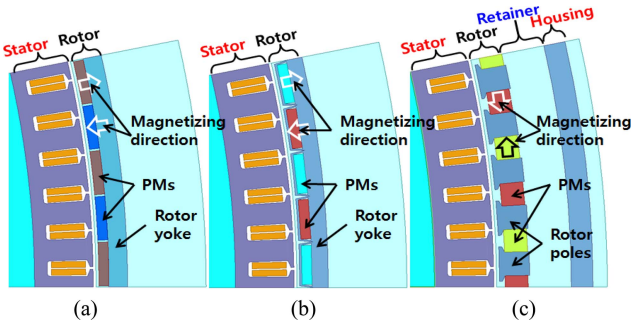

Fig. 2. (Color online) Three rotor topologies for 150P180S: (a) SPM rotor, (b) conventional IPM rotor, (c) spoke type IPM rotor.

Table 5. Comparison of current and torque according to rotor topology.

Topology / Performances	SPM rotor	Conventional IPM rotor	Spoke type IPM rotor
Current (A)	21.4	28.3	27.2
Torque (kNm)	5.7	5.6	5.8
Toq_cont (Nm/A)	266	198	213

Table 5 shows the computation results using 2-dimensional FEM for when the rotor topology was changed while maintaining the same rotor volume. As mentioned previously, the torque constant of an SPM rotor model is the highest, and the torque constant of the spoke-type IPM rotor model is better than that of the conventional IPM rotor model.

5. Decision of Outermost Dimensions

To compensate for the insufficient torque of the spoke-type IPM model, the outermost dimensions are changed.

5.1. Selection of Rotor Outer Diameter

Since the spoke-type rotor does not have a back-yoke, a non-magnetic material retainer is required between the rotor and rotor housing to reduce the leakage flux, as shown in Fig. 2(c). Fig. 3(a) shows the analysis results of the torque variation for changes in the retainer thickness. Since the torque variation is saturated when the retainer thickness is 20 mm, the rotor outer diameter is fixed at 1690 mm, considering both the motor housing and the retainer thickness.

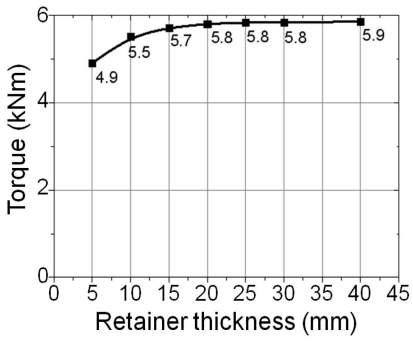

(a) torque to select rotor outer diameter

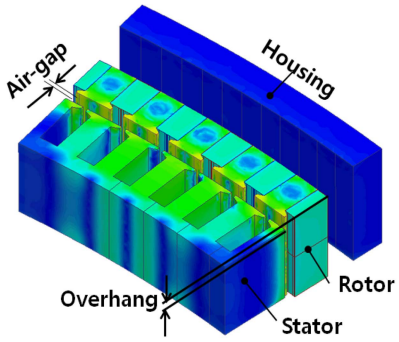

(b) 3-D FEA model to select axial length

Fig. 3. (Color online) Analysis results.

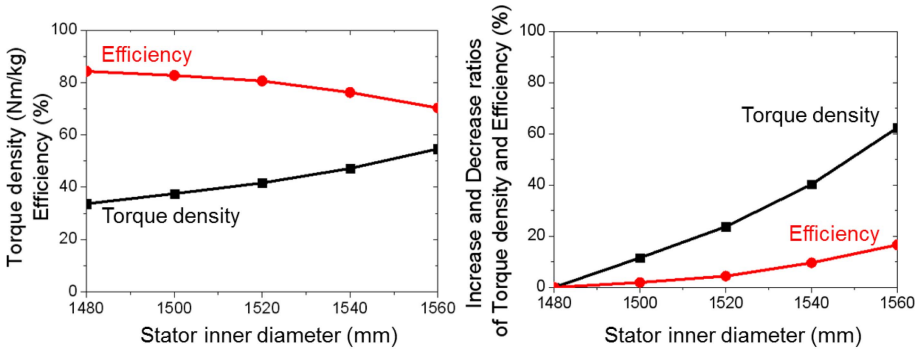

(a) torque density and efficiency (b) rate of change of (a)

Fig. 4. (Color online) Analysis results to select stator inner diameter.

5.2. Selection of Overhang Length

The core stack length is also examined to improve the torque value. While the variations of the inner and outer diameters are restricted by the specifications, the variation of the stack length is unrestricted. The stack length of the rotor core can afford the extension of the length of the end-coil thickness. To examine the overhang effect, a 3-dimensional (3-D) finite element analysis (FEA) model is used, as shown in Fig. 3(b). When the overhang length is increased by 16% (with rotor and stator core stack lengths of 58 mm and 50 mm, respectively, corresponding to an overhang length of 8 mm), the torque is improved by 12%. From now on, the overhang coefficient is considered to be 1.12 when the 2-D FEA is performed.

5.3. Selection of Stator Inner Diameter

To improve the efficiency, the stator inner diameter is examined. When the stator inner diameter is reduced, the slot area is relatively larger, and a conductor with wider area can be used. It is very effective to reduce copper loss, which is a major contributor to the total losses. Fig. 4(a) shows the analysis results of the efficiency and torque density variation according to the change of the stator inner diameter. The efficiency is appreciably changed, but the torque density variation is larger, as shown in Fig. 4(b). Therefore, the stator inner diameter is fixed at 1540 mm, and the effort to improve efficiency is continued in the optimum design process.

6. Discussions

Fig. 5 shows the 1/30 configuration of the examined model 150P180S, and its chosen dimensions. Additional information with analysis results is listed in the 'Fundamental design' column in Table 6. The optimum design results are also listed in the 'Optimal design' column. The

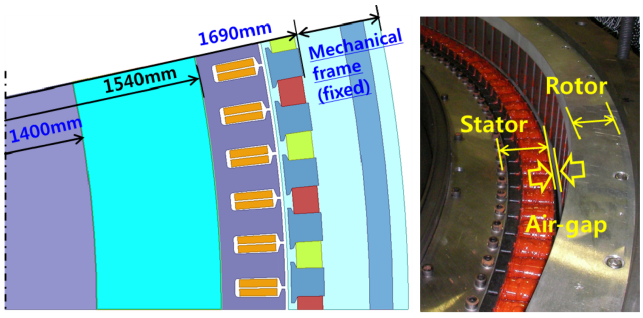

(a) analysis model (b) fabricated model

Fig. 5. (Color online) The configurations of analysis and fabricated model 150P180S.

used optimal design methodology is the same as that used by Hong *et al.* [3], and the variables considered and their boundaries are slightly different. The optimal results in this paper are introduced as prototype results in [3], where the process is second optimal design in the view point of whole design process. Comparing the results between the fundamental design and optimal design in Table 6, the efficiency looks like quite improved. However it is just because the magnetic materials are used for mechanical parts of the stator core fixing and it is reflected in analysis model of the only optimal design as shown in Fig. 6. It affects power improvement without any real dimension change. Except this material change, the changes of variables by the optimal design practically gave small variation in the motor performance. The measurement results are better than the design results, because the air-gap length is reduced. The air-gap length variation is due to the mechanical tolerance limitation in large-diameter systems.

This paper presented an initial motor design for turret without any specific optimal design process. Instead of using optimal design process, many assumptions and experienced techniques considering the large diameter are

Table 6. Comparison of design and measured results.

	Fundamental design	Optimal design	Measurement
Rotor outer diameter (mm)		1690	
Stator inner diameter (mm)	**1540**	**1528**	**1540-1528**
Air-gap length (mm)	4	4	3 ± 1
Stack length (mm)		50 / 80 (stator / rotor)	
No. of turn per phase		320 (6-parallel circuit)	
Stator tooth width (mm)	16	14.4	14.4 ± 0.01
Stator tooth height (mm)	28	31.9	31.9 ± 0.01
Wire diameter (mm)	**0.55**	**0.6**	**0.6**
Stator slot open width (mm)	2	3.51	3.51 ± 0.01
Rotor pole open width (mm)	8	9	9 ± 0.01
Current (A)	29	30.7	20.9
Resistance (ohm)	**3.18**	**2.1**	**2.2**
EMF constant (V/rpm)	10.79	10.97	10.94
Torque (kNm)	6.03	6.52	6.0
Torque constant (Nm/A)	208	212	287
Torque ripple (%)	1.2	1.7	2.4
Efficiency (%)	**68.6**	**74**	**74.8**

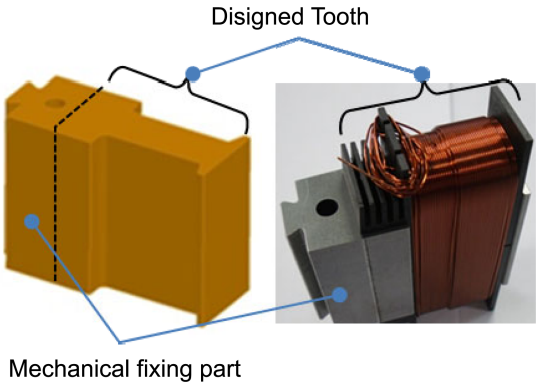

Fig. 6. (Color online) The configurations of fabricated stator tooth.

applied for simple and fast selection. The contents of this paper may be helpful for the initial design of machines with large diameter.

Acknowledgments

This work was supported by the Next Generation Military Battery Research Center program of Defense Acquisition Program Administration and Agency for Defense Development.

References

[1] S. Sadeghi and L. Parsa, IEEE Trans. Magn. **47**, 1658 (2011).
[2] J. Baek, S. Kwak, and H. A. Toliyat, J. Magnetics **18**, 65 (2013).
[3] D. Hong, J. Lee, B. Woo, D. Park, and B. Nam, IEEE Trans. Magn. **48**, 4491 (2012).
[4] J. Lee, D. Hong, B. Woo, K. Kim, and J. Hong, J. Magnetics **18**, 125 (2013).
[5] J. Lee, D. Koo, S. Moon, and C. Han, IEEE Trans. Magn. **48**, 2977 (2012).
[6] J. Lee, D. Hong, B. Woo, D. Park, and B. Nam, IEEE Trans. Magn. **48**, 915 (2012).
[7] A. Chen, R. Nilssen, and A. Nysveen, IEEE Trans. Ind. Appl. **46**, 779 (2010).
[8] F. Magnussen and C. Sadarangani, in Proc. IEEE IEMDC **1**, 333 (2003).
[9] Y. Kano and N. Matsui, IEEE Trans. Ind. Appl. **44**, 543 (2008).
[10] R. Wrobel and P. H. Mellor, IEEE Trans. Energy Conv. **23**, 1 (2008).
[11] J. Cros and P. Viarouge, IEEE Trans. Energy Conv. **17**, 248 (2002).
[12] F. Libert and J. Soulard, in Proc. ICEM, CD-ROM (2004).
[13] A. Wang, Y. Jia, and W. L. Soong, IEEE Trans. Magn. **47**, 3606 (2011).